

Beyond Mean Field: Fluctuation Diagnostics and Fixed-Point Behavior

Pok Man Lo

*Institute of Theoretical Physics, University of Wrocław, PL-50204 Wrocław, Poland**

We develop theoretical diagnostics for the breakdown of mean-field theory, demonstrate how spatial structure and finite interaction ranges enter the effective description, and show how these scales qualitatively modify the renormalization-group flow.

I. INTRODUCTION

Universality organizes critical phenomena through fixed points and scaling laws [1, 2], but it does not specify how close a system must be to a critical point before universal behavior becomes physically relevant. This is controlled by the size of the fluctuation-dominated region, which is non-universal and sensitive to microscopic details. In many systems—including those relevant to dense QCD matter—this region can be narrow, so identifying a universality class alone does not guarantee that critical behavior will be observable.

A more practical diagnostic comes directly from the Ginzburg–Landau (GL) framework. Within GL theory, the validity of mean-field (MF) solutions can be assessed by comparing fluctuation contributions to the MF order parameter, known as the GL criterion. This provides a quantitative measure of where fluctuations overwhelm MF behavior, without relying on universality arguments. Importantly, the criterion also applies to crossover transitions, making it broadly useful for realistic systems.

Fluctuation estimates can be further refined by retaining gradient terms in the GL functional. Standard Landau treatments often assume spatial homogeneity by neglecting these terms, an approximation commonly justified by the associated increase in kinetic energy. However, this assumption fails once non-local interactions are present, or more generally when quantum corrections are included. In such cases, spatially varying MF configurations arise naturally. Spatial structure is therefore not an exotic feature, but an intrinsic part of a consistent GL description and must be included in any reliable analysis.

Microscopic interactions may also introduce intrinsic momentum scales, which influence renormalization-group (RG) flows and the locations of fixed points. Understanding how model-dependent structures shape RG trajectories helps identify which features of an interaction kernel reorganize the effective theory at intermediate scales.

This article is intended as pedagogical notes that develop these ideas in a simple and transparent way. We focus on practical methods to quantify the breakdown of mean-field theory, assess the role of spatial structure, and analyze how RG flows respond to microscopic inputs.

II. REVISITING THE GINZBURG-LANDAU CRITERIA

The GL criterion focuses on the ratio

$$R_{\text{GL}} = \frac{\langle(\Delta\phi)^2\rangle}{\bar{\phi}^2}, \quad (1)$$

where ϕ is the order-parameter field and $\bar{\phi}$ its mean value. When $R_{\text{GL}} \gg 1$, fluctuations are no longer negligible and the MF approximation fails. In standard textbook treatments [1] this ratio is used to estimate the critical dimension. Here we take a different perspective: we use the criterion to identify the region in thermodynamic variables where MF theory does not apply. This region serves as a proxy for the extent of the fluctuation-dominated domain in the phase diagram.

We consider two ways to estimate $\langle(\Delta\phi)^2\rangle$. The first follows directly from the MF framework. Starting with the static susceptibility,

$$\begin{aligned} \chi_{\text{static}} &= \beta \int d^3x G_c(\vec{x}) \\ &= \beta \tilde{G}_c(\vec{k} = 0), \end{aligned} \quad (2)$$

where $G_c(\vec{x}) = \langle\phi(\vec{x})\phi(\vec{0})\rangle_c$ is the connected correlator and $\tilde{G}_c(\vec{k})$ its Fourier transform. Within MF theory the susceptibility reduces to

$$\chi_{\text{static}} \rightarrow U_{\text{MF}}''^{-1} = \left(\frac{\partial^2 U_{\text{MF}}(\phi)}{\partial\phi\partial\phi}\right)^{-1}, \quad (3)$$

leading to the MF expression for the GL ratio,

$$R_{\text{GL}}^{(1)} = \frac{\tilde{G}_c(\vec{k} = 0)}{V_\phi \bar{\phi}^2} = \frac{U_{\text{MF}}''^{-1}}{\beta V_\phi \bar{\phi}^2}. \quad (4)$$

Here V_ϕ denotes the region over which $\phi(x)$ can be approximated by its mean value. It should not be taken as infinite. In realistic situations the finite size of domains or the presence of gradient terms—unavoidable in the quantum case—limits the spatial extent over which a uniform field approximation is valid.

We illustrate the robustness of the GL ratio by examining a simple linear sigma model (LSM). The prototypical Landau potential is

$$U_{\text{LSM}}(\sigma) = -(1-t^2)\sigma^2 + \sigma^4 - h\sigma, \quad (5)$$

with $t = T/T_0$. Here T_0 is the only intrinsic scale of the model and is used as our unit of energy. The equation of

* pokman.lo@uwr.edu.pl

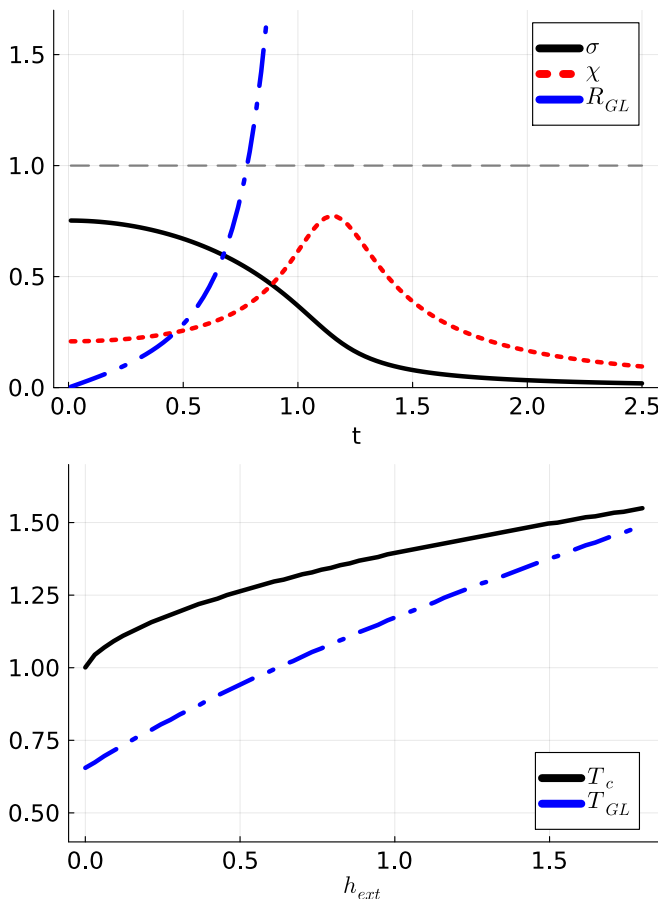


FIG. 1. Demonstration of the GL ratio in a linear sigma model. Top: temperature dependence at fixed explicit breaking h . Bottom: pseudo-critical temperature as a function of h . The interval $|T_{GL} - T_c|$ highlights the region where MF theory is not reliable.

motion can be solved numerically for arbitrary external field h , and the resulting mean field, static susceptibility, and GL ratio are shown in Fig. 1. In this example we set $V_\phi = 1$.

As the temperature increases, the GL ratio exceeds unity at a temperature T_{GL} that lies below the pseudo-critical temperature T_c , the latter identified from the peak of the static susceptibility. We further track the dependence of T_{GL} on the external field h and compare it with $T_c(h)$. The line of pseudo-critical temperatures plays the role of a phase diagram, while the area $|T_{GL} - T_c|$ quantifies the region where MF theory ceases to be reliable. As expected, this region widens when approaching the critical point, and the GL ratio provides a clean and quantitative diagnostic.

We now turn to an alternative and more general way of estimating fluctuations. Consider the fluctuation of the

field at a point:

$$\begin{aligned} G_c(\vec{x} \rightarrow \vec{0}) &= \lim_{\vec{x} \rightarrow 0} \langle \phi(\vec{x}) \phi(\vec{0}) \rangle_c \\ &= \int \frac{d^3k}{(2\pi)^3} \tilde{G}_c(\vec{k}). \end{aligned} \quad (6)$$

This quantity is dominated by UV momenta. To control this behavior, we define a regulated version,

$$G_c^\Lambda(\vec{0}) = \int^\Lambda \frac{d^3k}{(2\pi)^3} \tilde{G}_c(\vec{k}), \quad (7)$$

and construct the corresponding GL ratio

$$R_{GL}^{(2)}(\Lambda) = \frac{\int^\Lambda \frac{d^3k}{(2\pi)^3} \tilde{G}_c(\vec{k})}{\bar{\phi}^2}. \quad (8)$$

In this form, Λ is best interpreted as a physical scale specifying the range of fluctuations to be included—not as a UV cutoff intended to be removed. Misinterpreting it as such leads to unphysical conclusions.

At first sight, the definition above appears to be incompatible with the GL ratio in Eq. (4). We now show explicitly that no inconsistency exists. For illustration, we consider a simple Gaussian model with

$$\tilde{G}_c(\vec{k}) = \frac{1}{\beta} \frac{1}{\vec{k}^2 + m^2}. \quad (9)$$

The regulated integral can be evaluated analytically:

$$\int^\Lambda \frac{d^3k}{(2\pi)^3} \tilde{G}_c(\vec{k}) = \frac{1}{2\pi^2} \frac{1}{\beta} \left(\Lambda - m \tan^{-1} \frac{\Lambda}{m} \right). \quad (10)$$

The GL ratio in Eq. (4) probes long-wavelength fluctuations within a finite volume V . To reproduce the same low-momentum window, we choose $\Lambda = \Lambda_{IR}$ such that

$$\int^{\Lambda_{IR}} \frac{d^3k}{(2\pi)^3} = \frac{1}{V}, \quad (11)$$

which gives

$$\Lambda_{IR}^3 = \frac{6\pi^2}{V}. \quad (12)$$

Since Λ_{IR} is small, the leading-order expansion of Eq. (10) yields

$$\int^{\Lambda_{IR}} \frac{d^3k}{(2\pi)^3} \tilde{G}_c(\vec{k}) \approx \frac{1}{\beta m^2} \frac{1}{V}, \quad (13)$$

hence

$$R_{GL}^{(2)}(\Lambda_{IR}) \rightarrow \frac{\tilde{G}_c(\vec{k} \rightarrow 0)}{V \bar{\phi}^2}. \quad (14)$$

This matches the prescription of Eq. (4) and naturally explains the appearance of the $1/V$ factor.

This exercise teaches an important lesson: the two definitions of the GL ratio agree once they include the same physical range of fluctuations. Moreover, the regulated definition in Eq. (8) is often superior because it allows the IR fluctuation window to be tuned continuously.

Two remarks are in order. First, in textbook discussions the volume V_ϕ in Eq. (4) is often identified with the correlation volume $V_\xi = \xi^3$, with the correlation length estimated from the curvature of the MF potential,

$$\xi^2 \leftrightarrow U''_{\text{MF}}. \quad (15)$$

Away from the actual critical region this replacement is not valid. In particular, during a crossover the identification $V_\phi = V_\xi$ defeats the purpose of diagnosing the breakdown of MF theory.

Second, one might attempt to define a renormalized fluctuation by subtracting the UV contribution:

$$\begin{aligned} \langle \phi_R^2 \rangle_c &= \int^\Lambda \frac{d^3k}{(2\pi)^3} \beta^{-1} \left(\frac{1}{\vec{k}^2 + m^2} - \frac{1}{\vec{k}^2} \right) \\ &\rightarrow -\frac{m}{4\pi\beta}, \end{aligned} \quad (16)$$

where the limit $\Lambda \rightarrow \infty$ is finite. This procedure is equivalent to subtracting the correlator at $\xi = \infty \leftrightarrow m = 0$ suggested in Ref. [3]. In coordinate space this scheme corresponds to subtracting the UV singularity:

$$\begin{aligned} \langle \phi_R^2 \rangle_c &= G(\vec{x} \rightarrow 0) - G_{\text{bare}}(\vec{x} \rightarrow 0) \\ &= \beta^{-1} \lim_{r \rightarrow 0} \left(\frac{e^{-mr}}{4\pi r} - \frac{1}{4\pi r} \right) \\ &\rightarrow -\frac{m}{4\pi\beta}. \end{aligned} \quad (17)$$

Although this subtraction does remove the UV dependence, it produces the unphysical result that the square of an operator becomes negative. This is purely an artifact of the choice of a renormalization scheme—a finite correction ultimately linked to the choice of subtraction point.

A closely analogous issue arises in the renormalization of the Polyakov loop [4–6]. Expanding the loop,

$$\begin{aligned} \ell(x) &= \frac{1}{N_c} \text{tr} e^{i\beta A_4(x)} \\ &\approx 1 - \beta^2 \frac{1}{2N_c} \text{tr} A_4(x)^2 \\ &\approx \exp\left(-\frac{\beta^2}{2N_c} \text{tr} A_4(x)^2\right), \end{aligned} \quad (18)$$

one finds that certain renormalization schemes imply

$$\langle A_4^R(x)^2 \rangle < 0, \quad (19)$$

from which one would conclude that the renormalized Polyakov loop can exceed unity—contradicting the group-theoretic constraint restricting it to the target space parametrized by the Cartan angles [7], e.g. for $SU(3)$:

$$\ell = \frac{1}{3} \left(e^{i\gamma_1} + e^{i\gamma_2} + e^{-i(\gamma_1 + \gamma_2)} \right). \quad (20)$$

This remains a major conceptual issue in the theoretical treatment of the Polyakov loop [8]. Although the present discussion points toward a possible resolution, we set this issue aside and return to our main theme of developing methods that go beyond the standard MF treatment. In the next section we examine how to incorporate the kinetic term.

III. KINETIC TERM

We begin with a brief review of the GL formulation [1, 2, 9]. The partition function is written as a functional integral

$$Z_{\text{GL}} = \int D\phi_\Lambda e^{-\beta F_{\text{GL}}[\phi]}. \quad (21)$$

The relevant points are as follows: First, $F_{\text{GL}}[\phi]$ is the GL functional. We use F rather than H to emphasize that we are modeling a free-energy functional; the entropy contribution is absorbed into its coefficients.

Second, ϕ_Λ indicates that field configurations are restricted to be smooth up to a coarse-graining scale Λ , i.e. fluctuations with $p > \Lambda$ (or $L < \Lambda^{-1}$) have been integrated out. Schematically,

$$\begin{aligned} \phi_\Lambda(\vec{x}) &= \frac{1}{V} \sum_{\vec{x} \in \Lambda^{-3}} \phi(x) \\ &\rightarrow \int^\Lambda \frac{d^3k}{(2\pi)^3} \tilde{\phi}(\vec{k}) e^{i\vec{k} \cdot \vec{x}}. \end{aligned} \quad (22)$$

Third, Z_{GL} is a field-theoretic partition function: all compatible configurations are included, and the classical configuration satisfies

$$\frac{\delta F_{\text{GL}}}{\delta \phi} = 0. \quad (23)$$

Our aim here is to develop a framework that keeps the discussion as simple as Landau theory but includes the kinetic term explicitly. For this purpose we consider a classical model with a separable interaction kernel,

$$F_{\text{GL}}[\phi] = \int_{\vec{x}} \frac{1}{2} (\nabla\phi)^2 + \frac{\lambda_2}{2} \int_{\vec{x}, \vec{y}} V(\vec{x}, \vec{y}) \phi(\vec{x}) \phi(\vec{y}) + \frac{\lambda_4}{4} \left(\int_{\vec{x}, \vec{y}} V(\vec{x}, \vec{y}) \phi(\vec{x}) \phi(\vec{y}) \right)^2. \quad (24)$$

The equation of motion follows from

$$\frac{\delta F_{\text{GL}}}{\delta \phi(\vec{x})} = 0 = -\nabla^2 \phi(\vec{x}) + \lambda_2 \int_{\vec{y}} V(\vec{x}, \vec{y}) \phi(\vec{y}) + \lambda_4 \int_{\vec{y}} V(\vec{x}, \vec{y}) \phi(\vec{y}) \int_{\vec{x}', \vec{y}'} V(\vec{x}', \vec{y}') \phi(\vec{x}') \phi(\vec{y}'). \quad (25)$$

For a local kernel the problem reduces to the usual Landau theory. In general the classical configuration can be obtained numerically. To illustrate the structure analytically, and to contrast with the local case, we consider a separable kernel,

$$V(\vec{x}, \vec{y}) \rightarrow \bar{V} u(\vec{x}) u(\vec{y}). \quad (26)$$

The equation of motion becomes

$$-\nabla^2 \phi(\vec{x}) + (\lambda_2 \bar{V} c + \lambda_4 \bar{V}^2 c^3) u(\vec{x}) = 0, \quad (27)$$

where

$$c = \int_{\vec{x}} u(\vec{x}) \phi(\vec{x}), \quad (28)$$

and we define

$$Q = \lambda_2 \bar{V} c + \lambda_4 \bar{V}^2 c^3. \quad (29)$$

Thus,

$$\nabla^2 \phi(\vec{x}) = Q u(\vec{x}). \quad (30)$$

For definiteness we choose

$$u(\vec{x}) \rightarrow u(r) = e^{-m_1 r}, \quad (31)$$

where m_1 is a characteristic interaction scale. The solution is

$$\begin{aligned} \phi(\vec{x}) &= \frac{Q}{m_1^2} f(m_1 r), \\ f(x) &= \frac{e^{-x}(2+x)}{x}. \end{aligned} \quad (32)$$

The functional c becomes

$$\begin{aligned} c &= \int_0^\infty dr 4\pi r^2 u(r) \phi(r) \\ &= 3\pi \frac{Q}{m_1^5}. \end{aligned} \quad (33)$$

The self-consistency condition then fixes Q as

$$Q^2 = \frac{1 - \lambda_2 \bar{V} \frac{3\pi}{m_1^5}}{\lambda_4 \bar{V}^2 \left(\frac{3\pi}{m_1^5} \right)^3}. \quad (34)$$

TABLE I. Energy dimensions of model quantities

model quantity	energy dimension
F_{GL}	E
ϕ	E
λ_2	E^2
λ_4	E^3
$V(\vec{x}, \vec{y})$	E^3

This analytic model illustrates two points. First, interactions naturally generate a spatial profile for the classical field; here it is encoded in the function f . This already goes beyond the Landau picture, which concerns only the algebraic interplay between λ_2 and λ_4 . Second, a homogeneous configuration does not minimize F_{GL} . Using Eqs. (32) and (33), the functional reduces to

$$F_{\text{GL}}[\phi] \rightarrow F_{\text{MF}}(c) = -\frac{1}{2} \frac{m_1^5}{3\pi} c^2 + \frac{1}{2} \lambda_2 \bar{V} c^2 + \frac{1}{4} \lambda_4 \bar{V}^2 c^4, \quad (35)$$

where the first term originates from the kinetic contribution,

$$K = -\frac{1}{2} \int_{\vec{x}} \phi(\vec{x}) \nabla^2 \phi(\vec{x}). \quad (36)$$

This term lowers the free energy and invalidates the usual argument that a homogeneous configuration minimizes F_{GL} . Minimizing Eq. (35) reproduces Eq. (34).

It is well known that static MF descriptions fail near phase transitions, where fluctuations and dynamical critical behavior dominate [10, 11]. Even so, many QCD phase-diagram studies continue to employ spatially homogeneous MF models [12], which artificially produce discontinuous jumps in conserved densities—although real first-order interfaces are smooth and governed by gradient energy. When spatial dependence is included, it is usually limited to soliton-type models [13–15].

Our construction demonstrates that gradient terms arise naturally once interactions have finite range, making spatial structure an intrinsic part of the effective theory rather than an optional correction. The implications for finite-volume QCD and realistic system sizes—highlighted in finite-size scaling and endpoint studies [16–18]—remain to be clarified. Certain shapes

of an inhomogeneous background field can weaken first order phase transition to a crossover [19]. Phenomenological work on QCD droplets and nucleation has long recognized finite-size constraints [20], but droplet profiles are rarely solved dynamically in space.

IV. EVOLUTION OF FIXED POINTS

As a final topic we examine how RG flow equations are modified when an interaction introduces an inherent momentum scale. For concreteness we start from a conventional three-dimensional ϕ^4 model:

$$F_{\text{GL}}[\phi] = \int_{\vec{x}} \frac{1}{2} (\nabla\phi)^2 + \frac{\lambda_2}{2} \int_{\vec{x}} \phi^2 + \frac{\lambda_4}{4!} \int_{\vec{x}} \phi^4. \quad (37)$$

The RG flow tracks how the couplings (λ_2, λ_4) evolve as modes in the momentum shell $\Lambda \rightarrow \Lambda/b$ are integrated out, with $b = e^t$ and $t \rightarrow 0^+$. The derivation follows standard textbook treatments [1, 2, 21]; here we compute the one-loop momentum-shell calculation directly in $d = 3$, rather than using a $4 - \epsilon$ expansion with $\epsilon = 1$. The resulting flow equations are

$$\begin{aligned} \frac{d}{dt} \bar{\lambda}_2 &= 2\bar{\lambda}_2 + \frac{\bar{\lambda}_4}{4\pi^2} \bar{\beta}^{-1} \frac{1}{1 + \bar{\lambda}_2}, \\ \frac{d}{dt} \bar{\lambda}_4 &= \bar{\lambda}_4 - \frac{3}{4\pi^2} \bar{\lambda}_4^2 \bar{\beta}^{-1} \frac{1}{(1 + \bar{\lambda}_2)^2}, \end{aligned} \quad (38)$$

where the dimensionless parameters are

$$\bar{\lambda}_2 = \lambda_2/\Lambda^2, \quad \bar{\lambda}_4 = \lambda_4, \quad \bar{\beta} = \beta\Lambda. \quad (39)$$

The first term in each equation is the canonical scaling from the kinetic term, while the second originates from interactions.

Fixed points satisfy

$$\frac{d}{dt} \vec{\lambda} = \vec{0}, \quad \vec{\lambda} = \begin{pmatrix} \bar{\lambda}_2 \\ \bar{\lambda}_4 \end{pmatrix}. \quad (40)$$

There are two solutions: the Gaussian fixed point (GFP),

$$\vec{\lambda}_{\text{GFP}} = \begin{pmatrix} 0 \\ 0 \end{pmatrix}, \quad (41)$$

and the Wilson–Fisher fixed point (WFFP),

$$\vec{\lambda}_{\text{WFFP}} = \begin{pmatrix} -1/7 \\ \frac{48\pi^2}{49} \bar{\beta} \end{pmatrix}. \quad (42)$$

To characterize the local flow we evaluate the stability matrix,

$$\hat{W} = \frac{\partial}{\partial \vec{\lambda}} \left(\frac{d\vec{\lambda}}{dt} \right), \quad (43)$$

whose eigenvalues give the scaling directions. At the GFP,

$$\hat{W}_{\text{GFP}} = \begin{pmatrix} 2 & -\frac{1}{4\pi^2} \bar{\beta}^{-1} \\ 0 & 1 \end{pmatrix}, \quad (44)$$

with eigenvalues

$$v_{\text{GFP}} = [2, 1]. \quad (45)$$

At the WFFP,

$$\hat{W}_{\text{WFFP}} = \begin{pmatrix} 5/3 & \frac{7}{24\pi^2} \bar{\beta}^{-1} \\ \frac{16\pi^2}{7} \bar{\beta} & -1 \end{pmatrix}, \quad (46)$$

with eigenvalues

$$v_{\text{WFFP}} = \frac{1}{3} (1 \pm \sqrt{22}). \quad (47)$$

Positive (negative) eigenvalues correspond to repulsive (attractive) directions.

Separable Interaction

We now consider how a separable interaction modifies the flows. In momentum space we introduce a form factor

$$u(\vec{p}) = e^{-p^2/m_1^2}, \quad (48)$$

and replace only the quartic vertex by

$$F_4 \rightarrow \frac{1}{4!} \lambda_4 \int \prod_{i=1}^4 \frac{d^3 p_i}{(2\pi)^3} u_{p_i} \tilde{\phi}_{p_i} (2\pi)^3 \delta\left(\sum p_i\right). \quad (49)$$

This choice keeps the bookkeeping of internal and external lines in Feynman diagrams straightforward. Although the modification appears minimal, it corresponds in configuration space to a smeared two-body interaction rather than a strictly local one.

Because only the momentum shell contributes to the one-loop integrals, the flow equations acquire factors of

$$u_\Lambda = e^{-\Lambda^2/m_1^2}. \quad (50)$$

The modified flows are

$$\begin{aligned} \frac{d}{dt} \bar{\lambda}_2 &= 2\bar{\lambda}_2 + \frac{\bar{\lambda}_4}{4\pi^2} \bar{\beta}^{-1} \frac{u_\Lambda^2}{1 + \bar{\lambda}_2}, \\ \frac{d}{dt} \bar{\lambda}_4 &= \bar{\lambda}_4 - \frac{3}{4\pi^2} \bar{\lambda}_4^2 \bar{\beta}^{-1} \frac{u_\Lambda^4}{(1 + \bar{\lambda}_2)^2}. \end{aligned} \quad (51)$$

The GFP remains unchanged. The WFFP moves to

$$\vec{\lambda}_{\text{WFFP}} = \begin{pmatrix} -\frac{1}{1+6u_\Lambda^2} \\ \frac{4\pi^2}{3} \bar{\beta} \left(\frac{6u_\Lambda^2}{1+6u_\Lambda^2} \right)^2 \end{pmatrix}, \quad (52)$$

which reduces to Eq. (42) as $u_\Lambda \rightarrow 1$. In the opposite limit $u_\Lambda \rightarrow 0$ the fixed point is driven to $[-1, 0]$, which is not a genuine fixed point.

The stability matrix becomes

$$\hat{W}_{\text{WFFP}} = \begin{pmatrix} 5/3 & \frac{1}{4\pi^2} \bar{\beta}^{-1} f_u^{-1} \\ \frac{16\pi^2}{7} \bar{\beta} f_u & -1 \end{pmatrix}, \quad (53)$$

where

$$f_u = \frac{6u_\Lambda^2}{1 + 6u_\Lambda^2}. \quad (54)$$

A notable feature is that the eigenvalues remain unchanged as given in Eq. (47). We thus obtain a parametric class of theories that share the same universality class. In principle these theories can react to other energy scales like temperatures and densities differently.

Figure 2 shows the RG flow. The GFP (blue point) and WFFP (red star) are marked for reference. As expected, all trajectories move away from the GFP since both eigenvalues of its stability matrix are positive—it is fully repulsive. At the WFFP, one eigenvalue is negative, and the flow indeed approaches the fixed point along this stable direction. The form factor shifts the location of the WFFP and slightly rotates the flow, but the critical exponents, determined by the local eigenvalues, remain unchanged. If u_Λ allowed to run, the nontrivial fixed point eventually disappears and only the GFP survives.

These features reflect the simplicity of the separable interaction used here. It would be interesting to explore interaction kernels that modify not only the fixed-point location but also the corresponding stability eigenvalues, thereby providing a controlled way to generate tunable universality classes.

V. CONCLUSIONS

We have developed several theoretical ideas that go beyond the standard MF framework. Rather than emphasizing universality solely through fixed-point exponents, we focus on diagnostics that are directly tied to the actual behavior of the system.

Once gradient terms or finite-range interactions are included, spatial structure of the order parameter emerges naturally. Even minimal models generate nontrivial spatial profiles. This shows that spatial variation is not an exotic effect, but an intrinsic part of any consistent description beyond homogeneous mean-field theory.

Our RG analysis shows that introducing an intrinsic momentum scale through a separable interaction shifts the location of the nontrivial fixed point while leaving the critical exponents unchanged. This isolates which features of the interaction kernel affect RG trajectories. It also suggests that changing interaction range or nonlocality can, in more general settings, modify not only the fixed-point position but potentially the universality class itself.

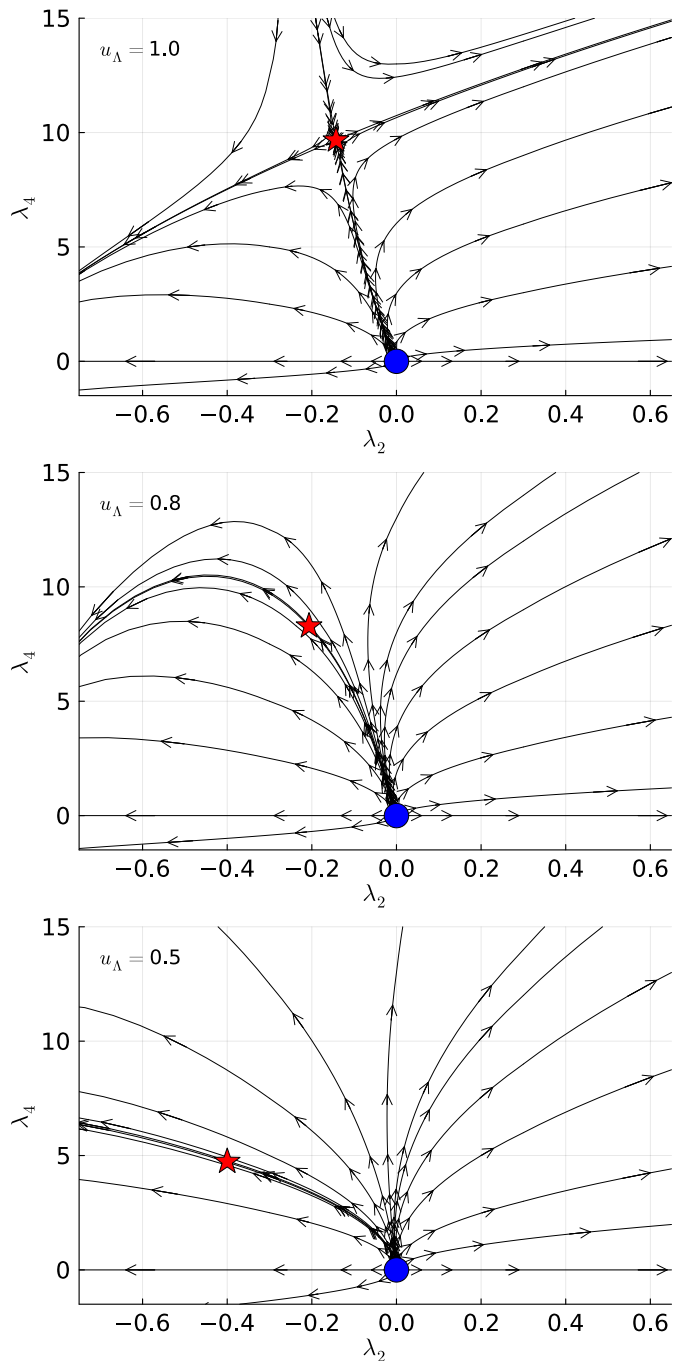


FIG. 2. RG flows for several values of u_Λ . The red star marks the WFFP and the blue point the GFP. Flows run away from the GFP (fully repulsive), while the WFFP features one attractive direction, allowing trajectories to approach it.

Ultimately, tools are only as useful as the problems they are applied to. The framework developed here sets the stage for studying interaction kernels motivated by QCD and other many-body systems, where finite-range effects, spatial inhomogeneities, and fluctuation windows are central ingredients. Such analyses can clarify which microscopic inputs control the emergence of universal be-

havior and where new universality structures may appear as interaction ranges or fluctuation scales are varied.

ACKNOWLEDGMENTS

The author thanks Song Shu and Thomas Klaehn for helpful comments. He acknowledges the Wrocław Centre for Networking and Supercomputing for providing accessible computational resources, as well as partial support from the Polish National Science Center (NCN) under Opus grant no. 2022/45/B/ST2/01527.

-
- [1] N. Goldenfeld, *Lectures on phase transitions and the renormalization group* (1992).
 - [2] J. L. Cardy, *Scaling and renormalization in statistical physics* (1996).
 - [3] B. Friman, C. Hohne, J. Knoll, S. Leupold, J. Randrup, R. Rapp, and P. Senger, eds., *The CBM physics book: Compressed baryonic matter in laboratory experiments*, Vol. 814 (2011).
 - [4] S. Nadkarni, Phys. Rev. D **33**, 3738 (1986).
 - [5] O. Kaczmarek, F. Karsch, P. Petreczky, and F. Zantow, Phys. Lett. B **543**, 41 (2002), arXiv:hep-lat/0207002.
 - [6] O. Kaczmarek and F. Zantow, Phys. Rev. D **71**, 114510 (2005), arXiv:hep-lat/0503017.
 - [7] P. M. Lo, K. Redlich, and C. Sasaki, Phys. Rev. D **103**, 074026 (2021), arXiv:2101.12663 [hep-ph].
 - [8] P. M. Lo, B. Friman, O. Kaczmarek, K. Redlich, and C. Sasaki, Phys. Rev. D **88**, 074502 (2013), arXiv:1307.5958 [hep-lat].
 - [9] K. Binder, Reports on Progress in Physics **50**, 783 (1987).
 - [10] P. C. Hohenberg and B. I. Halperin, Rev. Mod. Phys. **49**, 435 (1977).
 - [11] D. T. Son and M. A. Stephanov, Phys. Rev. D **70**, 056001 (2004).
 - [12] In astrophysical contexts, even a consistent MF model for a first-order QCD transition is still lacking, and some models previously claimed to describe deconfinement have been shown to be inconsistent [?].
 - [13] D. J. Gross, R. D. Pisarski, and L. G. Yaffe, Rev. Mod. Phys. **53**, 43 (1981).
 - [14] M. A. Escobar-Ruiz, E. Shuryak, and A. V. Turbiner, Phys. Rev. D **93**, 105039 (2016), arXiv:1601.03964 [hep-th].
 - [15] S. Shu, Sci. China Phys. Mech. Astron. **60**, 041021 (2017), arXiv:1607.01815 [nucl-th].
 - [16] J. Braun, B. Klein, and B.-J. Schaefer, Phys. Lett. B **713**, 216 (2012), arXiv:1110.0849 [hep-ph].
 - [17] L. F. Palhares, E. S. Fraga, and T. Kodama, Journal of Physics G: Nuclear and Particle Physics **38**, 085101 (2011).
 - [18] G. Kovács, P. Kovács, P. M. Lo, K. Redlich, and G. Wolf, Phys. Rev. D **108**, 076010 (2023), arXiv:2307.10301 [hep-ph].
 - [19] X. Li, S. Shu, and J.-R. Li, Phys. Rev. C **105**, 045203 (2022), arXiv:2108.12325 [hep-ph].
 - [20] E. S. Fraga and R. Venugopalan, Physica A **345**, 121 (2004), arXiv:hep-ph/0304094.
 - [21] A. Altland and B. Simons, *Condensed Matter Field Theory*, 3rd ed. (Cambridge University Press, 2023).